IEEE published version:

doi:10.1109/10.1109/SMC.2013.629

Driver Distraction Assessment Using Driver Modeling

Peter Hermannstädter and Bin Yang
Institute of Signal Processing and System Theory, University of Stuttgart, Stuttgart, Germany
{peter.hermannstaedter, bin.yang}@iss.uni-stuttgart.de

***Abstract*—Characterizing individual human drivers is of increasing interest for applications like adaptive driver assistance or monitoring. Describing the human driver by means of control-theoretic driver models constitutes a promising approach. In this paper, we apply a driver model adopted from literature to real-road driving of a distraction experiment in order to assess the driver state. The control-theoretic driver model features an anticipatory and a compensatory tracking component as well as a processing delay and a neuromuscular motor component. The distraction experiment data comprises real road driving with a visuomotor and an auditory secondary task, as well as reference driving. By means of prediction error identification, we continuously and individually estimate the model parameters from driving data of eleven drivers. We evaluate the distributions of the driver model parameters and the predictive capability of the estimated driver models. The estimated driver model parameters reflect distracted driving behavior according to the driving task. As a promising experimental result, the driver model parameters and predictive performance are significantly associated with driver distraction.**

***Index Terms*—Driver modeling, Driver distraction, Driver state, System identification, Driver monitoring, Fatigue, Intelligent vehicles, Vehicle safety, Automated driving**

I. Introduction

With driving safety, driver support, and automated driving in mind, the question of characterizing individual driving becomes an increasingly important task considering seamless interaction between humans and technical systems or adaptation of such systems to individuals. Few attempts have been made to apply control-theoretic driver modeling principles to applications such as driver state or driver distraction monitoring. However, control-theoretic driver models offer interesting opportunities, which may be advantageous in driver state detection, e.g. joint modeling of the human driver together with the driving task or an inherently time-related driver behavior description. This paper is part of a thorough investigation of the applicability of control-theoretic driver models to identify and capture variations in driver state as induced by attentional shifts, distraction or drowsiness.

In the field of driver modeling, a large number of driver modeling approaches from different research domains have been proposed for a variety of applications (see [1] for an overview). The proposed approaches in connection with driver support, to mention only a few, range from simple autoregressive modeling [2], [3], physiologically inspired modeling [4]–[8], to machine learning techniques [9], [10] and highly integrated and complex cognitive co-pilot systems [11]. However, among the literature regarding driver state detection (cf. [12]), few approaches employ driver modeling. For example, [10] proposes a modeling approach based on machine learning in connection with distracted driving classification, whereas [2], [3] use autoregressive models for lane keeping support.

Previous works indicate that varying driving behavior can be captured using control-oriented driver models. While [2] use an autoregressive model and show fatigue-related trends in the parameters and model residuals on driving simulator data, a preview driver model can also be used to capture varying steering behavior under real-world controlled driving conditions [13]. In this work, by employing the physiologically oriented driver model adopted from [6], [7] through system identification procedures to a real-world driving experiment with visuomotor and auditory distraction, we investigate the detection of driver distraction.

In Section II, we give an overview of the driver model from [6], [7] and of the computations to reconstruct perceptional and motor signals. Section III presents the system identification techniques as well as the identification and simulation scheme used in this paper. The real-world driving experiment with distractions by [14] from which the data originates is presented in IV. In Section V, analyses of the parameter identification quality (V-B), the distributions of the estimated parameters (V-C), and the model simulation performance are presented. In Section VI we conclude with the findings that the estimated parameters and the model simulation performance are sensitive to the induced distractions.

II. Cybernetic Driver Model

A large number of driver models for different applications have been published. In this paper, the model developed by Mars and Saleh [6], [7] has been selected due to its combination of perceptual and motor components.

A. Model Presentation

The model depicted in Figure 1 features an anticipatory and a compensatory tracking component, a processing time delay, and a neuromuscular subsystem with a torque control loop. Additionally, two aspects make this model especially useful for computational investigations: First, a thorough investigation of model parameters and their ranges is available in [7].

978-1-4799-0652-9/13/$31.00

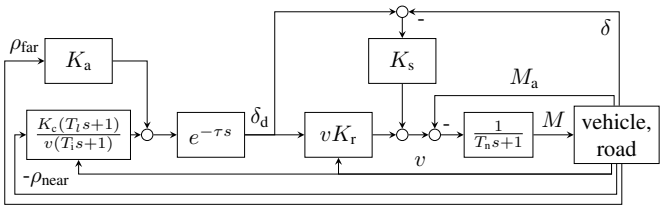

Fig. 1. Cybernetic driver model according to [6], [7] with visual system before the processing delay τ and a neuro-muscular system after the delay

Second, a closed-loop formulation of the driver-vehicle model is presented in [8] together with a full parameter set.

The driver model in Figure 1 shall now be thoroughly described in accordance with [6], [7]. As visual perception inputs it uses a *far point preview angle* ρ_{far} and a *near point preview angle* ρ_{near} (cf. Section II-B1 for a derivation). In the anticipatory part, ρ_{far} is amplified by the anticipation gain K_a. In the compensatory part, ρ_{near} is processed by a lead-lag-element $(T_l s+1)/(T_\text{i} s+1)$ with the time constants T_l, T_i and the compensation gain K_c scaled by the vehicle speed v. This is supposed to be a speed-dependent sensibility valid in the range of highway speeds. Anticipation and compensation signals are delayed by a processing time τ to form the intended steering wheel angle δ_d. Subsequently, this intention is modulated by the human neuromuscular system. δ_d is amplified by vK_r, which resembles the human internal model of the steering system. As an approximation of the human reflex system, the residual steering wheel angle between the intention δ_d and the steering wheel angle feedback δ, amplified by the steering stiffness coefficient K_s, is superimposed. Using the sensed steering alignment torque feedback M_a, a muscular control loop with neuromuscular time constant T_n is realized to generate the desired steering wheel torque M. Then, the single output of the model in Figure 1 is the acted steering wheel torque M. Note that although the model formulation is in continuous time, processing in the following is discrete with time index k.

B. Perceptional and Motoric Variables

In vehicle measurements from real road driving, the vehicle yaw angle $\psi_{\text{L},k}$ with respect to the lane and the lateral offset d_k from the lane center are available from lane tracking cameras. Standard vehicle sensors provide the vehicle speed v_k as well as the steering wheel angle δ_k. Thus, the perceived preview angles $\rho_{\text{near},k}$, $\rho_{\text{far},k}$, the steering wheel aligning torque $M_{\text{a},k}$, and the acted torque M_k have to be recomputed in order to be able to estimate the driver model parameters.

1) Preview Angles: As in [6], the near point angle $\rho_{\text{near},k}$ between the vehicle heading and a near point in the center of the lane at preview distance $l_\text{p} = 5\,\text{m}$ as well as the far or tangent point angle $\rho_{\text{far},k} = \rho_{\text{TP}}$ between the vehicle heading and the current lane tangent point are used as inputs. The near point angle is related to lane tracking behavior and the far point angle is related to previewing anticipatory steering behavior [15]. In the following, we compute the angles $\rho_{\text{near},k}$, $\rho_{\text{far},k}$, which Figure 2 visualizes.

a) Angle to Near Point: The near point preview angle ρ_{near} results from an approximation $\rho_{\text{near},k} \approx \psi_{\text{L},k} + \frac{d_k}{l_\text{p}}$, as illustrated in Figure 2(a). This approximation is valid for small angles $\psi_{\text{L},k}$ and approximately straight roads within distance l_p. Note that the coordinate conventions differ from [7].

b) Angle to Tangent Point: Computation of angle $\rho_{\text{far},k}$ is not trivial given complex road trajectories and only inertial and lane measurements of real driving data. As discussed in [13], we reconstruct the vehicle trajectory $\boldsymbol{p}_k$ from the vehicle yaw rate $\dot{\psi}_k$ and vehicle speed v_k at time instant k by

$$\psi_k = \sum_{i=0}^{k-1} T_\text{s}\dot{\psi}_i, \quad \boldsymbol{p}_k = \sum_{i=0}^{k-1} \underbrace{\begin{bmatrix}\cos\psi_i & -\sin\psi_i \\ \sin\psi_i & \cos\psi_i\end{bmatrix}}_{\mathbf{R}(\psi_k)} \begin{bmatrix}\Delta s_i \cos\frac{\Delta\psi_i}{2} \\ \Delta s_i \sin\frac{\Delta\psi_i}{2}\end{bmatrix}$$

where the inter-sample distance is $\Delta s_k \approx T_\text{s} v_k$ and the inter-sample yaw angle is $\Delta\psi_k = \psi_{k+1} - \psi_k \approx T_\text{s}\dot{\psi}_k$. With the current lane width w_k and with the assumption that d_k and w_k are measured perpendicular to the lane markings, the trajectories of the left and right lane markings $\boldsymbol{l}_k, \boldsymbol{r}_k$ of the vehicle's current lane can be reconstructed by

$$\boldsymbol{l}_k = \boldsymbol{p}_k + \mathbf{R}(\psi_k)\begin{bmatrix}0 & (\frac{w_k}{2} - d_k)\end{bmatrix}^T$$
$$\boldsymbol{r}_k = \boldsymbol{p}_k + \mathbf{R}(\psi_k)\begin{bmatrix}0 & (-\frac{w_k}{2} - d_k)\end{bmatrix}^T$$

Given $\boldsymbol{l}_k$ and $\boldsymbol{r}_k$, the angle $\rho_{\text{far},k}$ is determined from the observation that a tangent point within a previewed road window $i \in \{k, \ldots, k + N_{\text{prev}}\}$ can be located by finding the global, non-boundary extreme points $i_l = \arg\min_i \alpha_{l,i}$ and $i_r = \arg\max_i \alpha_{r,i}$ of all preview angles $\alpha_{l,i}$, $\alpha_{r,i}$ between the vehicle heading and any point $\boldsymbol{l}_k$, $\boldsymbol{r}_k$ respectively. Figure 2(b) illustrates this by the thick lines. After determining all visible i_l, i_r, the far point angle is chosen such that

$$\rho_{\text{far},k} = \begin{cases}\alpha_{l,i_l} & i_{\text{TP}} \in i_l \\ \alpha_{l,i_r} & i_{\text{TP}} \in i_r\end{cases}, \qquad i_{\text{TP}} = \max\{i_l, i_r\} \quad (1)$$

with i_{TP} the farthest visible tangent point in the preview window. This implements assumed human preview behavior. Conflicts in (1) are resolved to the smallest $\rho_{\text{far},k}$. For parallel lane markings, the tangent point is at infinite distance and $\rho_{\text{far},k}$ reduces to the lane yaw angle $\psi_{\text{L},k}$ of the vehicle. Finding $\rho_{\text{far},k}$ and current valid ρ_{TP} has to be repeated in every step k.

2) Steering Wheel Torques: The steering wheel torques $M_{\text{a},k}$, M_k are not available as vehicle signals in the data of this paper. Hence, they are reconstructed with a power steering model from [8], [16], on the one hand based on measurements

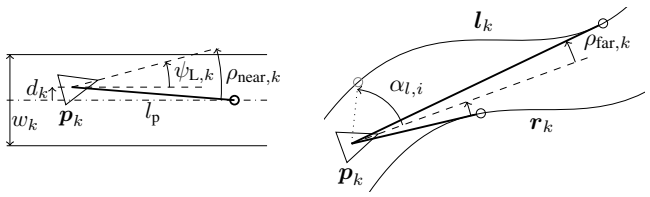

(a) Near point angle to road center (b) Far point angle to tangent point dotted: exemplary angle $\alpha_{l,i}$ to $\boldsymbol{l}_k$

Fig. 2. Preview angles to road center and to tangent point respectively

of vehicle yaw rate $\dot{\psi}_k$ and steering wheel angle signals δ_k, $\dot{\delta}_k$, on the other hand based on estimations of vehicle skid angle β_k and $\ddot{\delta}_k$ of the steering wheel angle δ_k. For this purpose, the β_k is using the well-known second order vehicle bicycle model (cf. e.g. [17]) and a Luenberger observer (cf. e.g. [18]), which will not be discussed here. Finally, using a numerical approximation of $\ddot{\delta}_k$ given measurements of $\dot{\delta}_k$, the torques M_k, $M_{\mathrm{a},k}$ are computed by evaluating the algebraic equations [7], [16]

$$M_{\mathrm{a},k} = \tfrac{l_f}{v} C_\mathrm{v} \dot{\psi}_k + C_\mathrm{v} \beta_k - \tfrac{1}{i_\delta} C_\mathrm{v} \delta_k$$
$$M_k = J_\delta \left(\ddot{\delta}_k - \tfrac{l_f}{v} C_\mathrm{v} \dot{\psi}_k - C_\mathrm{v} \beta_k + \tfrac{1}{i_\delta} C_\mathrm{v} \delta_k + \tfrac{\zeta_\delta}{J_\delta} \dot{\delta}_k \right)$$

with the coefficient $C_\mathrm{v} = \frac{2 c_f \eta K_\delta}{i_\delta J_\delta}$ and the parameters from Table I.

TABLE I
STEERING MODEL PARAMETERS (BASED ON MEASUREMENTS)

Parameter	Value	Description
c_f	86.61 kN/rad	front wheel cornering stiffness
l_f	1.4 m	center of gravity to front axle
η_f	0.07 m	tire patch length
i_s	15	steering transmission ratio
K_δ	0.19	manual steering column coefficient
J_δ	0.01 kg m^2	steering system moment of inertia
ζ_s	0.3	steering system damping coefficient

III. Identification of Driver Model Parameters

A. Parameter Estimation

To estimate the model parameters of the model depicted in Figure 1, we make use of the state space formulation thereof in [7]. The system equations are

$$\begin{aligned} \dot{\boldsymbol{x}}(t) &= \mathbf{A}(v)\boldsymbol{x}(t) + \mathbf{B}(v)\boldsymbol{u}(t) \\ \boldsymbol{y}(t) &= \mathbf{C}(v)\boldsymbol{x}(t) + \mathbf{D}(v)\boldsymbol{u}(t) \end{aligned} \tag{2}$$

with $v = v(t)$, $\boldsymbol{x}(t) = \begin{bmatrix} x_1(t) & x_2(t) & x_3(t) \end{bmatrix}^T$ the state vector, $\boldsymbol{y}(t) = \begin{bmatrix} M(t) & \delta(t) \end{bmatrix}^T$ the model output, and $\boldsymbol{u}(t) = \begin{bmatrix} \rho_\mathrm{far}(t) & \rho_\mathrm{near}(t) & \delta(t) & M(t) \end{bmatrix}^T$ the model input. Note that [7] also uses $\delta(t)$ as model output to improve convergence of the system identification. The matrices are

$$\mathbf{A}(v) = \begin{bmatrix} -\frac{1}{T_\mathrm{i}} & 0 & 0 \\ \frac{2K_\mathrm{c}}{v\tau}\left(\frac{T_l}{T_\mathrm{i}} - 1\right) & -\frac{2}{\tau} & 0 \\ -\frac{K_\mathrm{c}(vK_\mathrm{r}+K_\mathrm{s})}{vT_\mathrm{n}}\left(\frac{T_l}{T_\mathrm{i}} - 1\right) & \frac{2(vK_\mathrm{r}+K_\mathrm{s})}{T_\mathrm{n}} & -\frac{1}{T_\mathrm{n}} \end{bmatrix}$$
$$\mathbf{B}(v) = \begin{bmatrix} 0 & \frac{1}{T_\mathrm{i}} & 0 & 0 \\ \frac{2K_\mathrm{a}}{\tau} & \frac{-2K_\mathrm{c}T_l}{v\tau T_\mathrm{i}} & 0 & 0 \\ -\frac{K_\mathrm{a}(vK_\mathrm{r}+K_\mathrm{s})}{T_\mathrm{n}} & \frac{K_\mathrm{c}(vK_\mathrm{r}+K_\mathrm{s})}{vT_\mathrm{n}}\frac{T_l}{T_\mathrm{i}} & \frac{-K_\mathrm{s}}{T_\mathrm{n}} & -\frac{1}{T_\mathrm{n}} \end{bmatrix}$$
$$\mathbf{C}(v) = \begin{bmatrix} 0 & 0 & 1 \\ -\frac{K_\mathrm{c}}{v}\left(\frac{T_l}{T_\mathrm{i}} - 1\right) & 2 & 0 \end{bmatrix}$$
$$\mathbf{D}(v) = \begin{bmatrix} 0 & 0 & 0 & 0 \\ -K_\mathrm{a} & \frac{K_\mathrm{c}}{v}\frac{T_l}{T_\mathrm{i}} & 0 & 0 \end{bmatrix}.$$

TABLE II
STARTING VALUES, CONSTRAINTS AND DESCRIPTION OF THE DRIVER MODEL PARAMETERS [7]

Parameter	Value	Range	Description
K_a	3.4	$[0.05, 5]$	Anticipation gain
K_c	15	$[5, 50]$	Compensation gain
T_l	3	$[0.5, 5]$	Lead time constant
T_i	1	$[0.2, 4]$	Anticipation gain
τ	0.04	fixed	Processing delay
K_r	1	$[0.01, 1.5]$	Angle-to-torque internal model coeff.
K_s	12	$[0, \infty)$	Steering wheel holding stiffness
T_n	0.1	fixed	Neuromuscular time constant
l_p	5 m	fixed	Near-point preview length

This formulation requires approximation of the explicit time delay by a first-order Padé approximation. In order to process the driver model on sampled measurement data and to shorten processing time, equations (2) are discretized by

$$\begin{aligned} \mathbf{A}_T(v_k) &= T_\mathrm{s}\mathbf{A}(v) + \mathbf{I}, \qquad \mathbf{B}_T(v_k) = T_\mathrm{s}\mathbf{B}(v) \\ \boldsymbol{x}_{k+1} &= \mathbf{A}_T(v_k)\boldsymbol{x}_k + \mathbf{B}_T(v_k)\boldsymbol{u}_k \\ \boldsymbol{y}_k &= \mathbf{C}(v_k)\boldsymbol{x}_k + \mathbf{D}(v_k)\boldsymbol{u}_k \end{aligned} \tag{3}$$

which is justified by the short model sampling time $T_\mathrm{s} = 0.002$ compared to the system time constants greater than 0.02 s.

For system identification, we define the parameter vector $\boldsymbol{\theta} = [K_\mathrm{a}\ K_\mathrm{c}\ T_l\ T_\mathrm{i}\ K_\mathrm{r}\ K_\mathrm{s}]^T$, which comprises the identifiable parameters. The parameters τ, T_n and l_p are fixed to their nominal values. [7] argues that well-established values can be found in literature (cf. Table II).

The input-output data to fit the driver model to is composed from values recomputed in Section II-B or directly measured:

$$\boldsymbol{u}_k = \begin{bmatrix} \rho_{\mathrm{far},k} & \rho_{\mathrm{near},k} & \delta_k & M_{\mathrm{a},k} \end{bmatrix}^T, \quad \boldsymbol{y}_k = \begin{bmatrix} M_k & \delta_k \end{bmatrix}^T.$$

System identification uses the residual $\boldsymbol{\varepsilon}_i(\boldsymbol{\theta}) = \hat{\boldsymbol{y}}_i(\boldsymbol{\theta}) - \boldsymbol{y}_i$, where $\hat{\boldsymbol{y}}_i(\boldsymbol{\theta})$ is computed through integration of (3) over the identification window $i \in \mathcal{I} = \{k - N + 1, \ldots, k\}$. All initial conditions are set to zero. The identification problem to find the best parameter vector $\hat{\boldsymbol{\theta}}$ for this window is then stated as

$$\epsilon_\mathcal{I}(\boldsymbol{\theta}) = \frac{1}{N} \sum_{i \in \mathcal{I}} (\boldsymbol{\varepsilon}_i(\boldsymbol{\theta}))^T \boldsymbol{\varepsilon}_i(\boldsymbol{\theta}) \tag{4}$$

$$\hat{\boldsymbol{\theta}} = \arg\min_{\boldsymbol{\theta}} \epsilon_\mathcal{I}(\boldsymbol{\theta}), \tag{5}$$

B. Identification and Validation Scheme

Constrained prediction error identification as implemented by the System Identification toolbox of MATLAB 8.0 is used to identify model parameters. The parameter vector $\hat{\boldsymbol{\theta}}$ is estimated based on the criterion (5) in an *output error* approach [19] and no disturbance model is estimated. The nominal parameter values from [7] are used as starting values. The constraints have been modified to accommodate the different vehicle and experiment setting. Table II shows the values, constraints, and meanings.

Identification is conducted on a window basis across a drive regardless of the distraction task as Figure 3 depicts. The identification windows are denoted by $\mathcal{I}$. An identified model

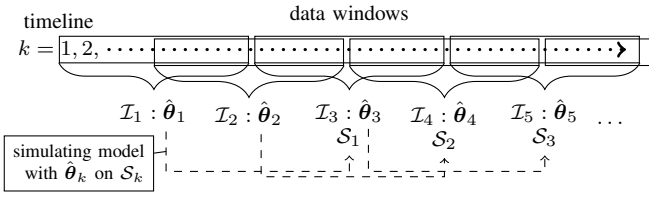

Fig. 3. Per-driver scheme of identification and simulation partitioning of data (identification window $\mathcal{I}$, simulation window $\mathcal{S}$; dashed: corresponding windows for identification and simulation)

is then validated on the next subsequent, non-overlapping window denoted by $\mathcal{S}$, as indicated by the dashed lines in Figure 3. On $\mathcal{S}$, the predictive model performance $\epsilon_{\mathcal{S}}(\boldsymbol{\theta})$ is computed according to (4). In the following, the distributions of the identified model parameters and the evaluated predictive model performance are analyzed with respect to the distraction tasks.

IV. Driver Distraction Experiment

The data set[1] used for the analysis in this paper has been collected as part of the driver monitoring study presented in [14] that investigates EEG-based neurological measures related to attention and distraction. In the real-road driving experiment, the subjects had to perform an auditory and a visuomotor secondary task during real road driving.

A. Route and Measurements

The experiment was conducted on the German Autobahn A81 south of the city of Stuttgart. Throughout the distraction experiment, adaptive cruise control was activated for safety reasons and the drivers were not allowed to overtake. Additionally, all drives were accompanied by supervisors trained in identification and intervention of safety-critical situations, for which the vehicle was equipped with extra pedals at the passenger seat. In this paper, data of $N = 14$ drivers is examined. These drives have been conducted with a 2009 Mercedes-Benz E-Class. In this vehicle, sensor measurements are available from off-the-shelve sensors comprising lane tracking camera, adaptive cruise control radar, yaw rate, and odometry sensors, recorded at a sampling time of $0.02\,\mathrm{s}$.

B. Distraction Tasks

After an initial driving stage to familiarize themselves with the vehicle and the adaptive cruise control functionality, the drivers had to complete a visuomotor and an auditory secondary task, as well as phases of driving without any applied distraction. For the purpose of this paper, a short description of the distraction tasks is given. Refer to [14] for a thorough description and neurophysiological evaluation.

The *visuomotor distraction* consisted of a Landolt ring (c-shaped symbols) task presented on a separate display in the vehicle at the location approximately of the radio console. Four Landolt rings were presented in a 2-by-2 configuration with one ring orientated differently from the others. Using two buttons comfortably placed on the vehicle's middle console, the drivers had to enter the column of the odd Landolt ring. After an input, a different set of Landolt rings was presented. Each of the visuomotor distraction tasks lasted for 3 minutes. Referring to the driving performance examined in this paper, the drive segments with visuomotor distraction are considered to induce severe visual distraction with a significant number of eye glances off road and considerable non-smooth out-of-the-loop effects regarding the driver vehicle control loop.

After the visuomotor distraction task, the participants completed a segment of $1.5\,\mathrm{min}$ of *undistracted driving* before starting with the auditory task.

The *auditory distraction* consisted of listening to a German audiobook and identifying the German article word "die". For each identified word, participants had to push a button. The button was attached to their left index finger tip such that the button operation did not interfere with the steering wheel operation nor involve visual inspection. Each of the auditory task segments had a duration of 3 minutes. After each segment, the drivers had to answer a question related to the content of the audiobook chapter they had listened to. For the purpose of this paper, the auditory distraction segments are considered to occupy attentional resources which might affect situation perception. However, at the same time the task is not considered to induce eye glances off the road.

After the auditory distraction task, the participants completed another segment of $1.5\,\mathrm{min}$ of undistracted driving.

The sequence *visuomotor task – undistracted driving – auditory task – undistracted driving* was completed four times in a row by every participant.

TABLE III
Driving data statistics

	Vehicle speed v (m/s)	Lane lateral offset d (m)	Steering wheel angle δ (rad)
average median	28.417	-0.061	0.008
average standard dev.	0.376	0.168	0.017

V. Results

A. Experiment Data

All investigations in the following are based on a moving window of 500 data samples ($10\,\mathrm{s}$) with a window shift of 250 samples ($5\,\mathrm{s}$). Inapplicable windows with data such as lane changes, inaccurate lane signals, or large accelerations have been discarded. For this resulting dataset, the statistics in Table III have been computed. On every window, a median and standard deviation value have been computed and subsequently averaged over all windows to give an impression of the data.

B. Parameter Identification

The data set for system identification of driver models is composed from the recorded vehicle sensor measurements using the reconstruction of perceptional and motoric variables from Section II.

[1]Courtesy of Daimler AG

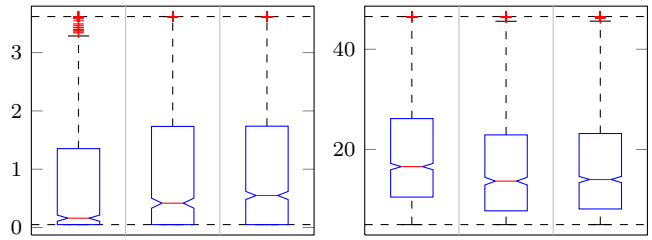

(a) Anticipation gain K_a (b) Compensation gain K_c

Fig. 4. Boxplots of two out of six identified model parameters (Boxes: lower and upper bound 25% and 75% percentiles; contained line: median; notches: median confidence region; whiskers span approx 95% of data; outlier marks +, clipped at dashed lines)

Identification preprocessing involved removal of sample means, filtering of the data window using a lowpass filter with cutoff frequency of 5 rad/s to focus on the frequency range of interest in manual control tasks [20] and first-order-hold upsampling to the model sampling rate $T_\mathrm{s} = 0.002\,\mathrm{s}$.

On $N = 4049$ windows, driver models have been identified according to Section III with v_k set to the median vehicle speed over the window. The identification quality has been assessed and outliers have been excluded, which may originate e.g. from small, untracked situational changes or numerical identification artifacts. Thresholds have been defined for the identification MSE $\epsilon_{\mathcal{I},k}(\hat{\boldsymbol{\theta}})$ when exceeding the 98%-percentile and for the normalized error

$$\breve{\boldsymbol{\epsilon}}_{\mathcal{I},k}(\hat{\boldsymbol{\theta}}) = \begin{bmatrix} \frac{|\hat{\delta}_k(\boldsymbol{\theta}) - \delta_k|}{|\hat{\delta}_k(\boldsymbol{\theta}) - \bar{\delta}_I|} & \frac{|\hat{M}_k(\boldsymbol{\theta}) - M_k|}{|\hat{M}_k(\boldsymbol{\theta}) - \bar{M}_I|} \end{bmatrix}^T$$

where $\bar{\delta}_I, \bar{M}_I$ denote the sample mean of δ_k, M_k over the identification window $\mathcal{I}$. Valid models have to fulfill these thresholds on both $\mathcal{I}$ and $\mathcal{S}$ intervals. After exclusion, the total number of models is $N = 3864$, distributed across the groups at $N_\mathrm{undistr.} = 1469$, $N_\mathrm{auditory} = 1456$, $N_\mathrm{visual} = 939$.

C. Driver Distraction

The identified driver models are analyzed in the three task groups visuomotor distraction, auditory distraction, and undistracted driving.

In the following the two fundamental approaches of analyzing identified driver models are employed: First, the distributions of the *model parameters* identified across the identification windows $\mathcal{I}$ (Figure 3) are analyzed with respect to the task groups. Second, the *model simulation performace* is evaluated accross the simulation windows $\mathcal{S}$ (Figure 3) for its predictive capability compared to measured driver behavior.

1) Model Parameters: Figure 4 shows boxplots of the anticipation and the compensation gains K_a, K_c out of six estimated model parameters with respect to the task groups. The figure reveals the dependence of the identified driver model parameters on the distraction tasks. Visual distraction results clearly in different parameters than auditory distraction or undistracted driving, whereas the latter two show very similar distributions. In the visual distraction tasks, the compensation gain K_c is larger compared to other task, while the anticipation gain K_a is smaller. This corresponds to the expected behavior in a visually demanding distraction task, which involves more corrective steering effort and less planned ahead action. However, variations of the parameters within the task groups are much larger than the differences across the task groups. Still, using the statistical Kruskal-Wallis test (rank-based ANOVA) and multiple comparision adjustment, discrimination between the task groups is possible for the parameters K_a, K_c and T_l with the statistical significance value p at a significance level of 0.05, as listed in Table IV.

TABLE IV
DISCRIMINATION ANALYSIS OF THE MODEL PARAMETERS WITH RESPECT TO GROUPS OF DISTRACTED AND UNDISTRACTED DRIVING

Comparisons[a]	Parameters and p-Values					
	K_a <0.001	K_c <0.001	T_i 0.0701	T_l <0.001	K_r 0.0730	K_s 0.1668
vis./undist.	*	*	-	*	-	-
vis./aud.	*	*	-	-	-	-
undist./audi.	-	-	-	*	-	-

[a] Significant distinctions at $p < 0.05$ marked with *

To individualize the assertions of the model parameters with respect to the distraction tasks, a baselining scheme has been employed. For each driver, individual baselining of the identified parameters was undertaken by subtracting the respective medians in undistracted driving from the parameters values during the distraction tasks. However, this had no considerable effect on the delimitation of the distraction tasks by the parameters and thus is not discussed here.

2) Model Simulation Performance: Contrary to the evaluation of the model parameter distributions, the predictive model performance is evaluated on the simulation windows $\mathcal{S}$ of the data (cf. Figure 3). The MSE $\epsilon_{\mathcal{S},k}$ is computed similarly to (4) between a model's simulation result and the measured data from $\mathcal{S}$. Figure 5 shows the distributions across all the three driving task groups and suggests pairwise discrimination of all three task groups. Using again a Kruskal-Wallis rank-based ANOVA and adjustment for multiple comparisons, the task groups show statistically significant differences with $p < 0.001$. The model performance also shows expected deterioration during visual distraction due to the intermittent nature of the secondary task, which repeatedly interrupts

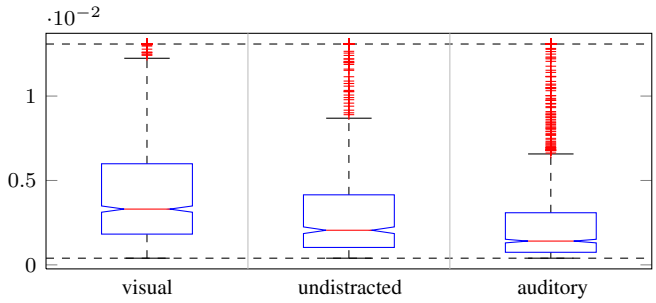

Fig. 5. Discrimination of distraction tasks from undistracted driving using the model simulation error MSE $\epsilon_{\mathcal{S},k}$ on simulation segments $\mathcal{S}$

the driver-vehicle control loop. Remarkably, the predictive model performance improves in the auditory distraction tasks compared to undistracted driving. A reason for this might be that the actual lane keeping improves and the driver behavior becomes more similar to the lane tracking controller behavior of the model as the driver's visual focus concentrates at the central road scene during the auditory task. Effects like these have been reported from driving studies in connection with lane keeping during phone conversations [21] and eye gaze distribution under mental load [22].

VI. Conclusion and Future Work

In this paper we employed an approach to analyze distracted and undistracted driving using a control theoretic driver model with physiological aspects from literature. We successfully analyzed the identified model parameter distributions as well as the predictive model performance for effects associated with distraction tasks.

Differences in the distribution of the model parameters as well as the predictive model performance are statistically significant between driving undistractedly or with a visual or auditory secondary task. The anticipation and compensation gains $K_\mathrm{a}, K_\mathrm{c}$ reflect expected human behavior in the visual distraction task compared to undistracted driving and show a shift in steering behavior from anticipatory towards compensatory control. The predictive model performance evaluated by computing the model simulation MSE on simulation data is the only feature showing significant differences between all three driving tasks. As expected, the predictive performance decreases under visual distraction compared to undistracted driving. The increased performance under auditory distraction is surprising but explicable: it might be related to more continuous human lane tracking control as the driver focuses more on the road ahead due to less visual activity under auditory load [21], [22].

The explained results show good interpretability. However, further work will have to examine to what extent the estimation procedure uniquely identifies model parameters and thus facilitates relating parameter values to the modeled phenomenons. Moreover, this study evaluates parameters over a population of drivers. An individualization attempt to baseline each driver's model parameters with respect to his or her individual undistracted driving data could provide no further information. Achieving a better individualization to account for individual driving styles and to improve individual over whole population distraction assessment is also subject to further research towards an actual detection system.

The presented approach of identifying model parameters from driving data and deriving measures from the parameter distributions and the predictive model performance is also subject to further improvements regarding predictive application of a model to multiple other drive segments. Constrained iterative parameter estimation currently consumes a lot of processing power and shows slow convergence. Other approaches using high-order identification in a first step and order reduction and model fitting in a second step are to be evaluated.

Computational demand is also a question of interest regarding in-vehicle applications. In the long range, this work is to be extended to other kinds of driver state supervision and driver characterization with an eye to the increasing demand for driver-centered supervision, assistance, and automation.

References

[1] M. Plöchl and J. Edelmann, "Driver models in automobile dynamics application," *Vehicle Syst. Dyn.*, vol. 45, no. 7, pp. 699–741, 2007.

[2] T. E. Pilutti and A. G. Ulsoy, "Identification of driver state for lane-keeping tasks," *IEEE Trans. Syst., Man, Cybern. A*, vol. 29, no. 5, pp. 486–502, 1999.

[3] M. Shi, "Real time human driver identification for improved safety," Ph.D. dissertation, University of California, Berkeley CA, 2008.

[4] A. J. Pick and D. J. Cole, "Neuromuscular dynamics in the driver–vehicle system," *Vehicle Syst. Dyn.*, vol. 44, no. sup1, pp. 624–631, 2006.

[5] M. Mulder, D. A. Abbink, and E. R. Boer, "Sharing Control With Haptics: Seamless Driver Support From Manual to Automatic Control," *Hum. Factors*, 2012.

[6] F. Mars, L. Saleh, P. Chevrel, F. Claveau, and J.-F. Lafay, "Modeling the Visual and Motor Control of Steering With an Eye to Shared-Control Automation," *Proc. Hum. Fact. Ergon. Soc. Annu. Meet.*, pp. 1422–1426.

[7] L. Saleh, P. Chevrel, F. Mars, J. Lafay, and F. Claveau, "Human-Like Cybernetic Driver Model for Lane Keeping," *IFAC World Congress*, vol. 18, no. 1, pp. 4368–4373, 2011.

[8] L. Saleh, P. Chevrel, F. Claveau, J.-F. Lafay, and F. Mars, "Shared Steering Control Between a Driver and an Automation: Stability in the Presence of Driver Behavior Uncertainty," *IEEE Trans. Intell. Transport. Syst.*, vol. 14, no. 2, pp. 974–983, 2013.

[9] C. Miyajima, Y. Nishiwaki, K. Ozawa, T. Wakita, K. Itou, K. Takeda, and F. Itakura, "Driver modeling based on driving behavior and its evaluation in driver identification," *Proc. IEEE*, vol. 95, no. 2, pp. 427–437, 2007.

[10] T. Ersal, H. J. A. Fuller, O. Tsimhoni, J. L. Stein, and H. K. Fathy, "Model-Based Analysis and Classification of Driver Distraction Under Secondary Tasks," *IEEE Trans. Intell. Transport. Syst.*, vol. 11, no. 3, pp. 692–701, 2010.

[11] X. Fu, H. H. Mosebach, D. Gamrad, K. Lemmer, and D. Söffker, "Modeling And Implementation Of Cognitive-Based Supervision and Assistance," in *Mathmod Conference 2009*, Wien, 2009. [Online]. Available: http://elib.dlr.de/58096/1/Mathmod_paper_090107.pdf

[12] Y. Dong, Z. Hu, K. Uchimura, and N. Murayama, "Driver Inattention Monitoring System for Intelligent Vehicles: A Review," *IEEE Trans. Intell. Transport. Syst.*, vol. 12, no. 2, pp. 596–614, 2011.

[13] P. Hermannstädter and B. Yang, "Identification and validation of lateral driver models on experimentally induced driving behavior," pp. 1165–1170, 2012.

[14] A. Sonnleitner, M. Simon, W. E. Kincses, and M. Schrauf, "Assessing driver state - Neurophysiological correlates of attentional shift during real road driving," *Hum. Factors*, (to appear).

[15] D. D. Salvucci and R. Gray, "A two-point visual control model of steering," vol. 33, no. 10, pp. 1233–1248, 2004.

[16] T. Raharijaoana, "Commande robuste pour l'assistance au contrôle latéral d'unm véhicule routier," Ph.D. dissertation, Université Paris Sud - Paris XI, Paris, 2004. [Online]. Available: http://tel.archives-ouvertes.fr/tel-00721986/

[17] D. Schramm, M. Hiller, and R. Bardini, *Modellbildung und Simulation der Dynamik von Kraftfahrzeugen*. Berlin and Heidelberg: Springer, 2010.

[18] J. Lunze, *Regelungstechnik 2*, 5th ed., ser. Springer-Lehrbuch. Berlin and Heidelberg and New York: Springer, 2008.

[19] L. Ljung, *System identification : theory for the user*, 2nd ed. Upper Saddle River and NJ [u.a.]: Prentice Hall, 2006.

[20] G. Johannsen, H. E. Boller, E. Donges, and W. Stein, *Der Mensch im Regelkreis: Lineare Modelle*, 1st ed., ser. Methoden der Regelungstechnik. München and Wien: Oldenbourg, 1977.

[21] K. A. Brookhuis, G. d. Vries, and D. d. Waard, "The effects of mobile telephoning on driving performance," *Accident Anal. Prev.*, vol. 23, no. 4, pp. 309–316, 1991.

[22] M. Sodhi, B. Reimer, and I. Llamazares, "Glance analysis of driver eye movements to evaluate distraction," *Behav. Res. Meth. Ins. C.*, vol. 34, no. 4, pp. 529–538, 2002.